

Electronic Supplementary Information for

**N-methyl-2-pyrrolidone as an Excellent Coordinative Additive with a Wide  
Operating Range for Fabricating High-Quality Perovskite Films**

Fangwen Cheng,<sup>†</sup> Xiaojing Jing,<sup>†</sup> Ruihao Chen, Jing Cao, Juanzhu Yan, Youyunqi Wu,  
Xiaofeng Huang, Binghui Wu\* and Nanfeng Zheng\*

State Key Laboratory for Physical Chemistry of Solid Surfaces, Collaborative  
Innovation Center of Chemistry for Energy Materials, and Engineering Research Center  
for Nano-Preparation Technology of Fujian Province, College of Chemistry and  
Chemical Engineering, Pen-Tung Sah Institute of Micro-Nano Science and Technology,  
Xiamen University, Xiamen 361005, China.

E-mails: binghuiwu@xmu.edu.cn; nfzheng@xmu.edu.cn. Fax: +86-592-2183047.

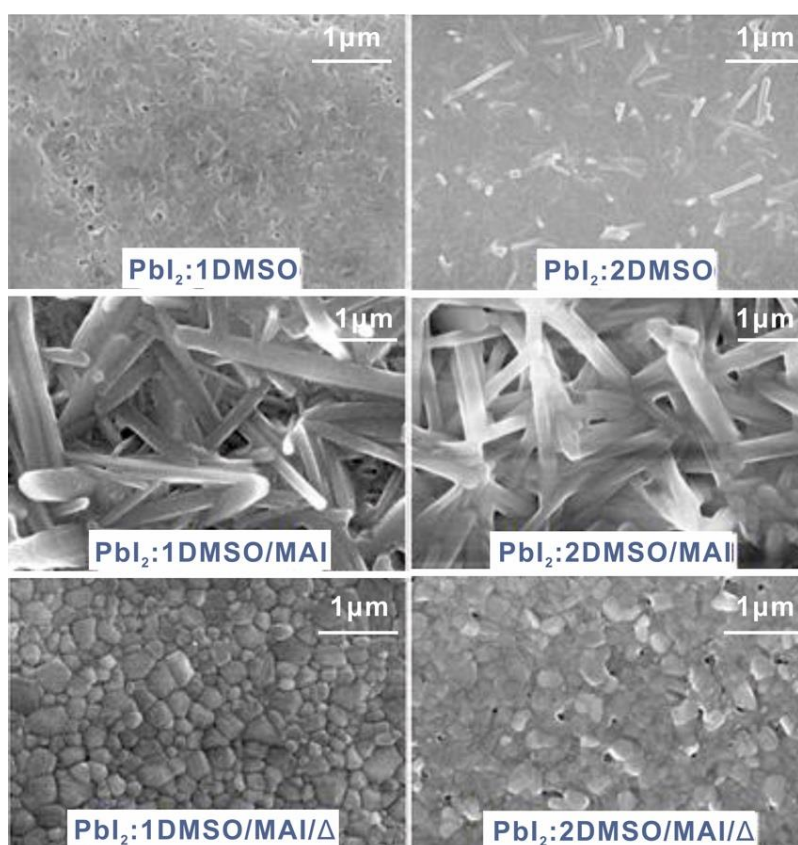


**Figure S1.** SEM images of  $\text{PbI}_2$  precursor films and the reaction with MAI before and after annealing ( $\Delta$ ) prepared with  $\text{PbI}_2/\text{DMSO}$  molar ratios of 1:1 and 1:2.

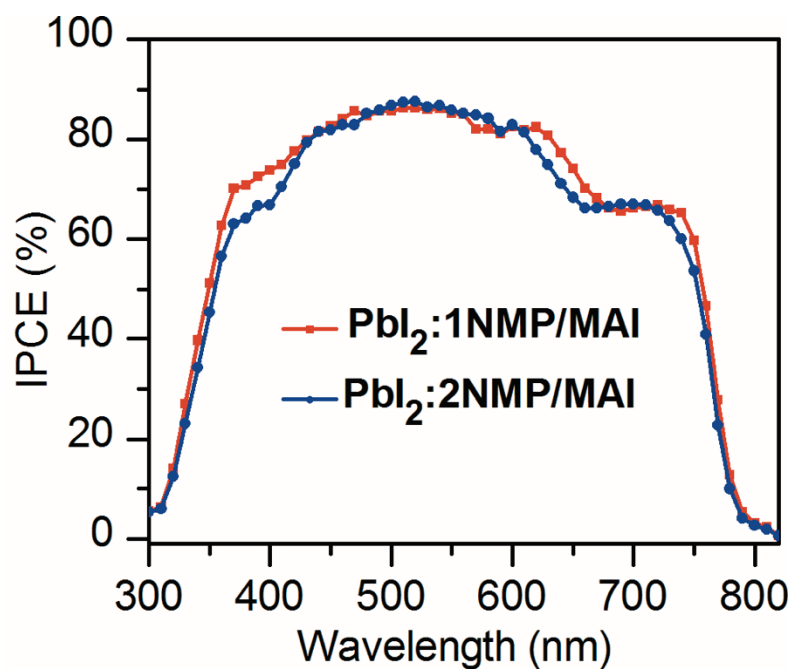


**Figure S2.** Best IPCE characteristics of perovskite films prepared with  $\text{PbI}_2/\text{NMP}$  molar ratios of 1:1 and 1:2.

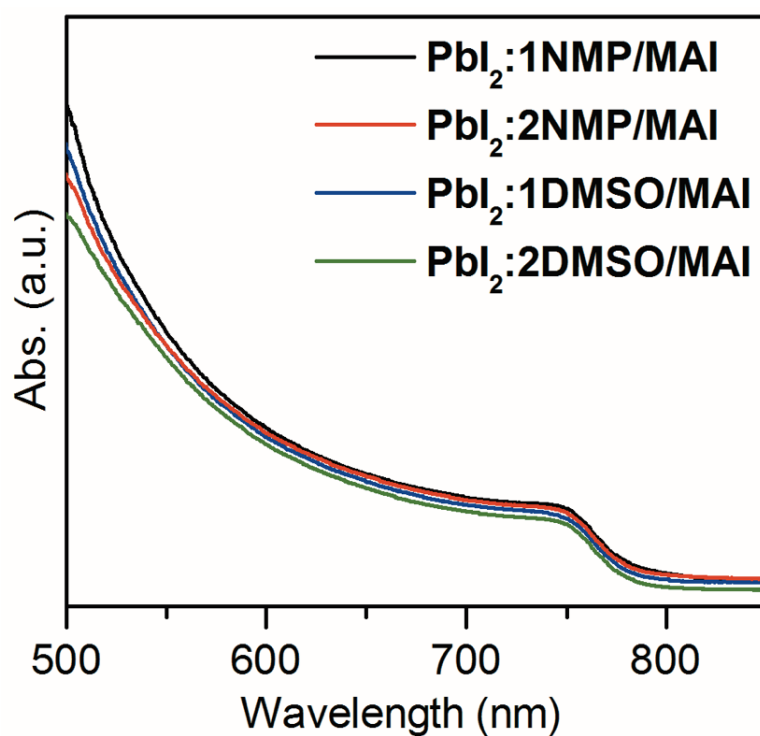


**Figure S3.** UV-vis absorption spectra of perovskite films prepared with different  $\text{PbI}_2/\text{NMP}$  ratios.

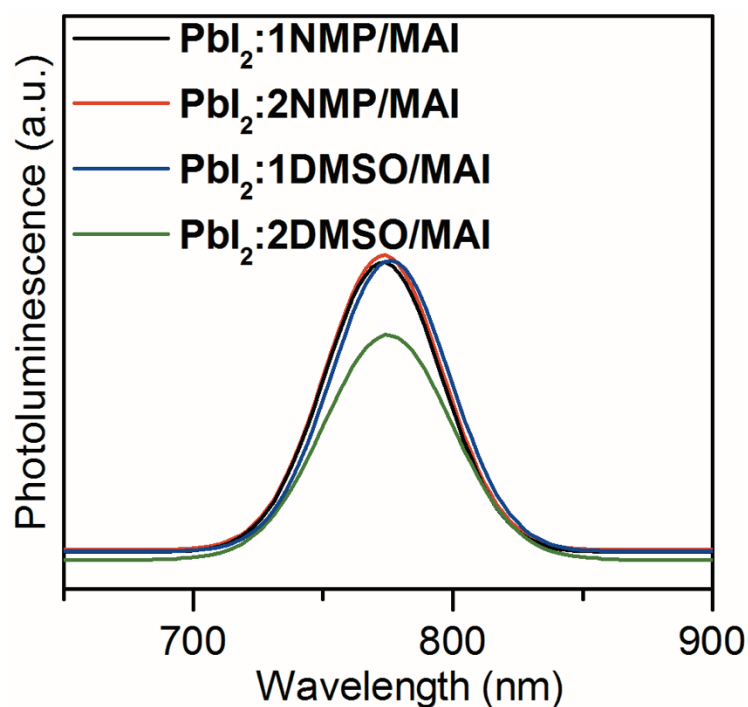


**Figure S4.** Steady-state photoluminescence spectra of perovskite films prepared with different  $\text{PbI}_2/\text{NMP}$  ratios. The quality of perovskite films made from NMP showed no dependence on  $\text{PbI}_2/\text{NMP}$  ratio, however, the  $\text{PbI}_2/\text{DMSO}$  ratio obviously affected the the quality of as-prepared perovskite films.

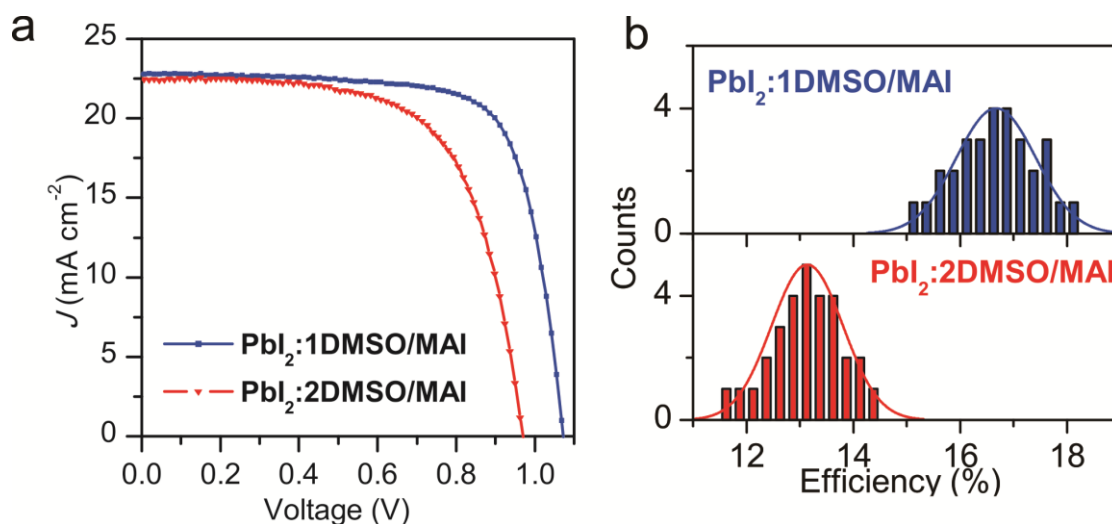


**Figure S5.** (a) Best  $J$ - $V$  characteristics and (b) histograms of efficiencies among 30 cells of PSC devices with  $\text{PbI}_2/\text{DMSO}$  molar ratios of 1:1 and 1:2.

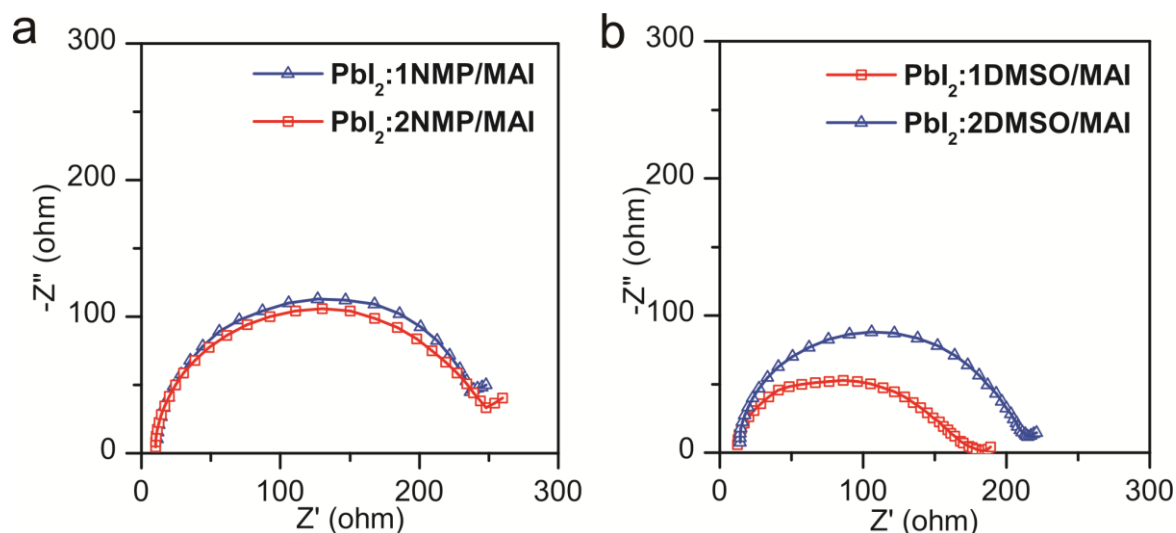


**Figure S6.** Electrical impedance spectroscopies (EIS) at 0 V bias under one sun illumination on whole devices with different perovskite layers: (a) PbI<sub>2</sub>:1NMP and PbI<sub>2</sub>:2NMP; (b) PbI<sub>2</sub>:1DMSO and PbI<sub>2</sub>:2DMSO. These impedances refer to the charge recombination rates in perovskite films.

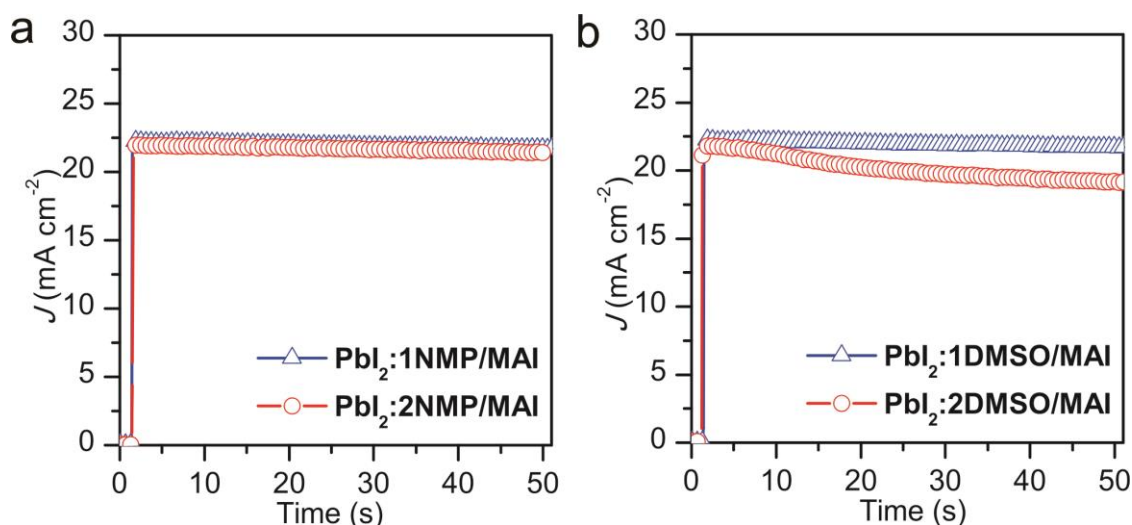


**Figure S7.** Stabilized outputs of current density measured as a function of time for devices fabricated with (a) PbI<sub>2</sub>:1NMP and PbI<sub>2</sub>:2NMP at their maximum power points (0.89 V bias and 0.88 V bias, respectively) and (b) PbI<sub>2</sub>:1DMSO and PbI<sub>2</sub>:2DMSO at their maximum power points (0.88 V bias and 0.82 V bias, respectively). The output of PbI<sub>2</sub>:1NMP, PbI<sub>2</sub>:2NMP and PbI<sub>2</sub>:1DMSO devices maintained stable over 50 s, which was in good agreement with the *J-V* tests. In contrast, the PbI<sub>2</sub>:2DMSO devices continuously degraded probably due to the presence of pinholes in the perovskite film (Figure S1).

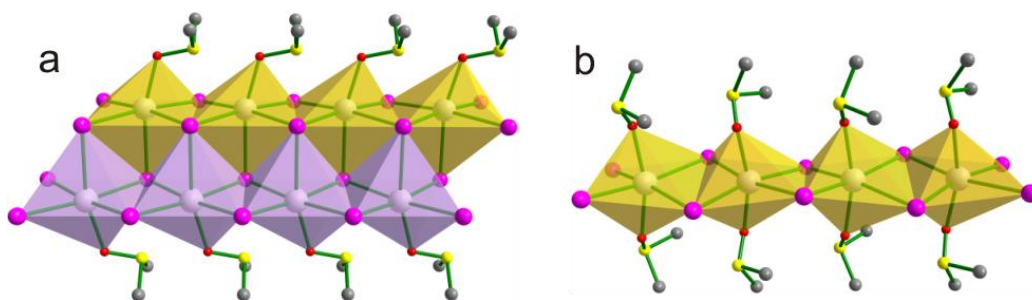


**Figure S8.** Crystal structure of (a)  $\text{PbI}_2 \cdot \text{DMSO}$  and (b)  $\text{PbI}_2 \cdot 2\text{DMSO}$ .

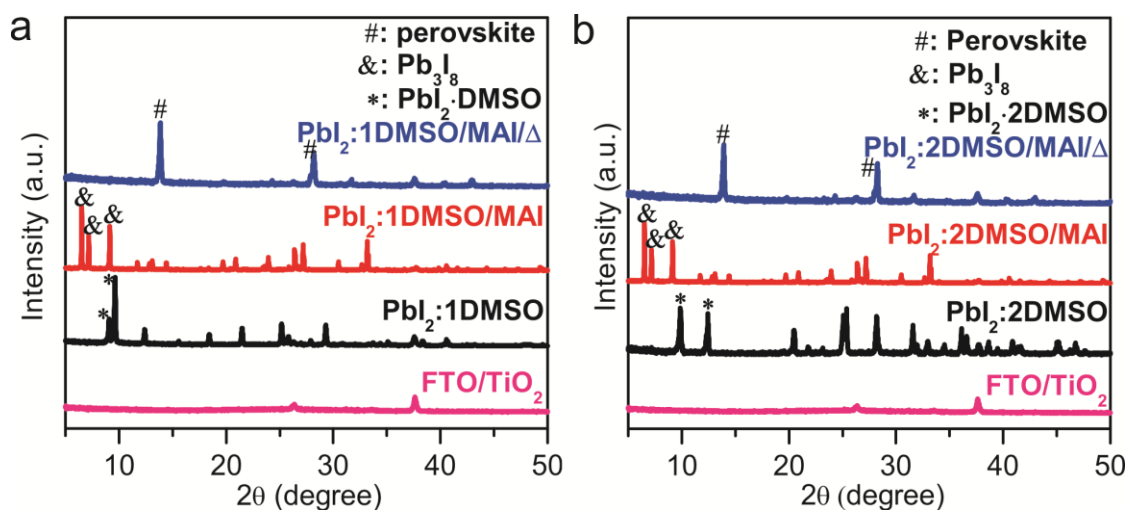


**Figure S9.** XRD patterns of the precursor films and the perovskite films (before and after annealing  $\Delta$ ) in the case of (a)  $\text{PbI}_2:1\text{DMSO}$  and (b)  $\text{PbI}_2:2\text{DMSO}$ .

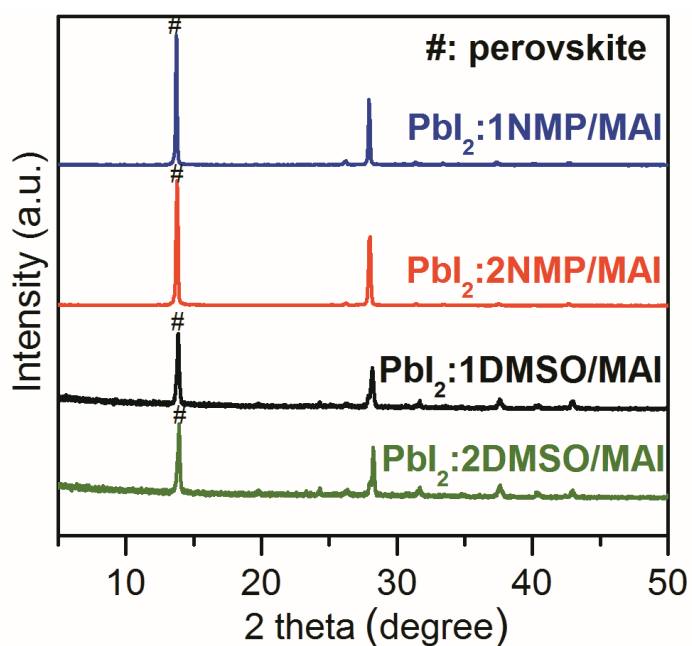


**Figure S10.** XRD patterns of the perovskite films deposited with  $\text{PbI}_2:1\text{NMP}$ ,  $\text{PbI}_2:2\text{NMP}$ ,  $\text{PbI}_2:1\text{DMSO}$  and  $\text{PbI}_2:2\text{DMSO}$ .

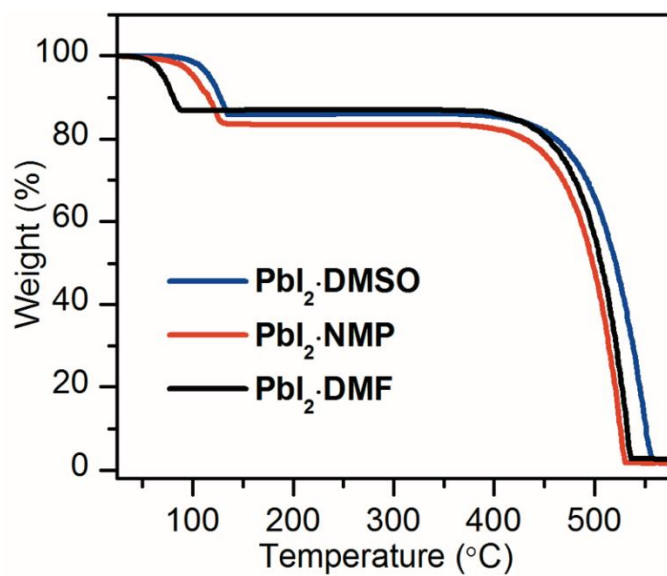


**Figure S11.** TGA curves of  $\text{PbI}_2 \cdot \text{DMF}$ ,  $\text{PbI}_2 \cdot \text{NMP}$  and  $\text{PbI}_2 \cdot \text{DMSO}$  powder samples.

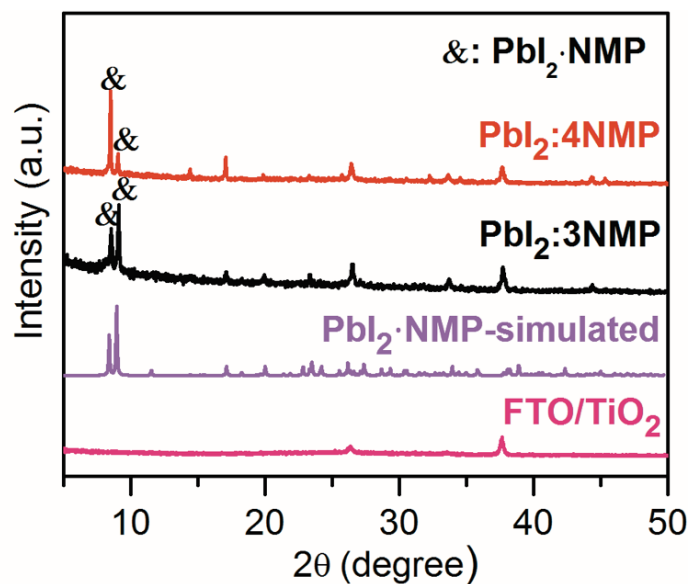


**Figure S12.** Comparison of simulated and experimental XRD patterns of precursor films prepared with  $\text{PbI}_2/\text{NMP}$  molar ratios of 1:3 and 1:4.

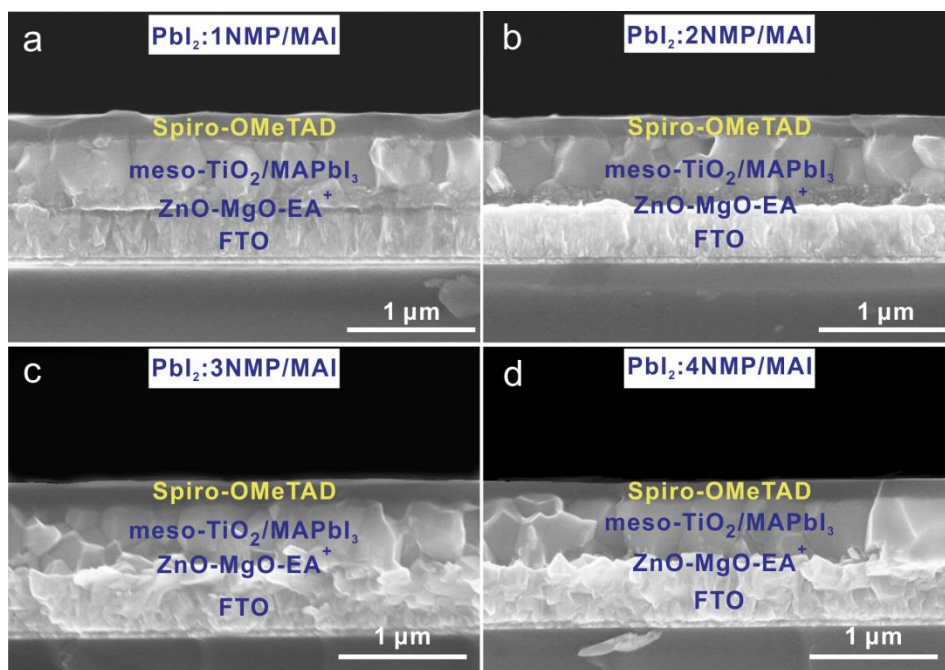


**Figure S13.** Cross-sectional SEM images of devices fabricated with  $\text{PbI}_2/\text{NMP}$  molar ratios of (a) 1:1, (b) 1:2, (c) 1:3 and (d) 1:4.

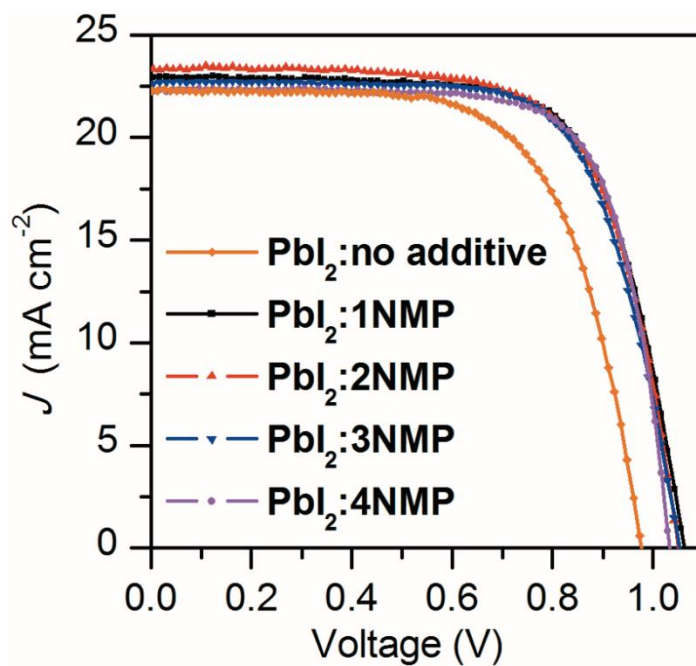


**Figure S14.**  $J$ - $V$  characteristics of  $\text{MAPbI}_3$  PSCs fabricated with different  $\text{PbI}_2/\text{NMP}$  ratios (from 1:0 to 1:4).



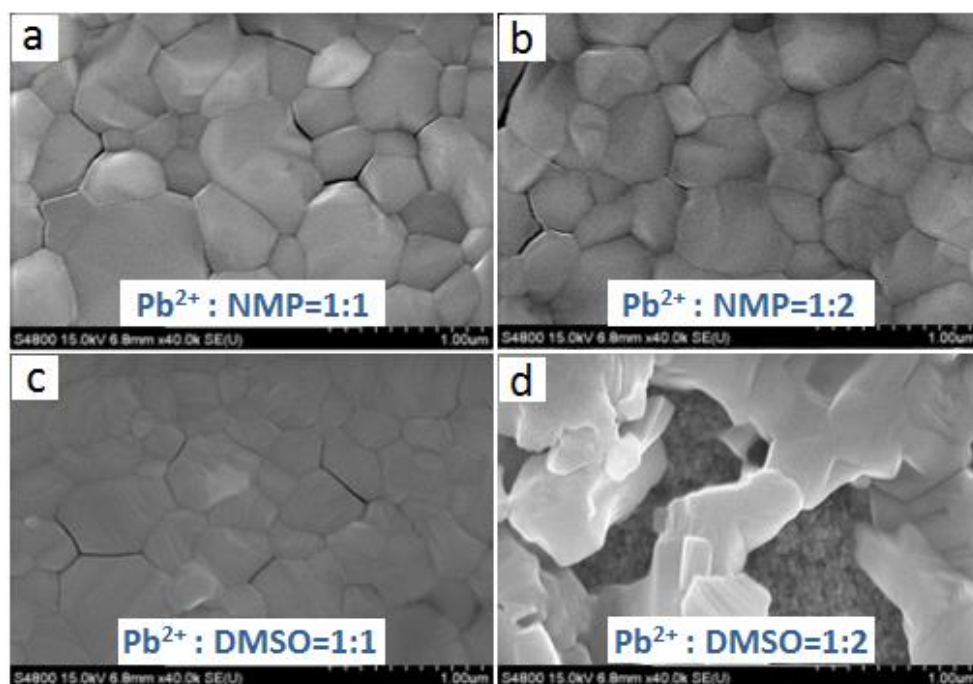


**Figure S15.** SEM images of Cs/FA/MA perovskite films prepared with  $\text{Pb}^{2+}$ /NMP molar ratios of (a) 1:1 and (b) 1:2 and  $\text{Pb}^{2+}$ /DMSO molar ratios of (c) 1:1 and (d) 1:2.

**Table S1.** Photovoltaic parameters of the champion cells with different molar ratios of  $\text{PbI}_2$ /NMP and different fabricated methods.

Devices	$J_{sc}/\text{mA}\cdot\text{cm}^{-2}$	$V_{oc}/\text{V}$	$FF/\%$	$\eta/\%$	$R_s/\Omega\cdot\text{cm}^{-2}$
$\text{PbI}_2$ :1NMP/MAI	23.5	1.07	75.6	19.1	3.41
$\text{PbI}_2$ :2NMP/MAI	23.5	1.06	77.1	19.2	3.90
$\text{Pb}^{2+}$ :1NMP/CsI-FAI-MABr	24.5	1.07	76.5	20.1	3.36
$\text{Pb}^{2+}$ :2NMP/CsI-FAI-MABr	24.5	1.06	76.8	20.1	3.66



**Table S2.** Crystal data and structure refinement for PbI<sub>2</sub>·NMP.

Complexes	PbI <sub>2</sub> NMP
Formula	C <sub>5</sub> H <sub>9</sub> I <sub>2</sub> NOPb
M/g mol <sup>-1</sup>	560.12
T/K	100.01(10)
Crystal system	Monoclinic
Space group	<i>P2/m</i>
<i>a</i> /Å	4.6337(2)
<i>b</i> /Å	19.1129(8)
<i>c</i> /Å	12.1265(5)
$\alpha$ /deg	90
$\beta$ /deg	98.144(4)
$\gamma$ /deg	90
<i>V</i> /Å <sup>3</sup>	1063.13(8)
<i>Z</i>	4
<i>d</i> <sub>cal</sub> /g cm <sup>-3</sup>	3.499
Limiting indices	-5 ≤ <i>h</i> ≤ 6, -23 ≤ <i>k</i> ≤ 24, -15 ≤ <i>l</i> ≤ 11
Reflections collected / unique	2422/2177 [ <i>R</i> ( <i>int</i> ) = 0.0655]
Goodness-of-fit on <i>F</i> <sup>2</sup>	1.049
Final <i>R</i> indices [ <i>I</i> > 2σ( <i>I</i> )]	<i>R</i> <sub><i>I</i></sub> = 0.0564 <i>wR</i> <sub>2</sub> = 0.1386